The 2009 IEEE/RSJ International Conference on
Intelligent Robots and Systems
October 11-15, 2009 St. Louis, USA

Self-adapting Robot Arm Movement Employing Neural Oscillators

Woosung Yang, Ji-Hun Bae, Jaesung Kwon, Nak Young Chong, Younghwan Oh and Bum Jae You, *Member*, *IEEE*

Abstract— **This paper proposes a neural oscillator based control to attain rhythmically dynamic movements of a robot arm. In human or animal, it is known that neural oscillators could produce rhythmic commands efficiently and robustly under the changing task environment. In particular, entrainments of the neural oscillator play a key role to adapt the nervous system to the natural frequency of the interacted environments. Hence, we discuss how a robot arm controls for exhibiting natural adaptive motions as a controller employing the entrainment property. To demonstrate the excellence of entrainment, we implement the proposed control scheme to a real robot arm. Then this work shows the performance of the robot arm coupled to neural oscillators in various tasks that the arm traces a trajectory. Exploiting the neural oscillator and its entrainment property, we experimentally verify an impressive capability of self-adaptation of the neural oscillator that enables the robot arm to make adaptive changes corresponding to an exterior environment.**

I. Introduction

Human and animal surprisingly exhibit adaptive or robust behaviours against unexpected disturbances or environment changes. This is because that the musculo -skeletal system is activated like a mechanical spring by means of the central pattern generators (CPGs) and their entrainment property [1]-[3]. The CPGs consist in the neural oscillator network and produce a stable rhythmic signal. Entrainment of the neural oscillator plays a key role to adapt the nervous system to the natural frequency of the interacted environments incorporating a sensory feedback. Hence, more interests on the artificial neural oscillator coupled to robot dynamics have been increasing in the field of biologically inspired robots to be deployable to real-world environments. The neural oscillator in the nervous system offers a potential controller, since it is known to be robust and have an entrainment characteristic as a general controller.

Relating these previous works, the mathematical description of a neural oscillator was presented in Matsuoka's works [1]. He proved that neurons generate the rhythmic patterned output and analyzed the conditions necessary for the steady state oscillations. He also investigated the mutual inhibition networks to control the frequency and pattern [2], but did not include the effect of the feedback on the neural oscillator performance. Employing Matsuoka's neural oscillator model, Taga *et al*. investigated the sensory signal from the joint angles of a biped robot as feedback signals [3], [4], showing that neural oscillators made the robot robust to the perturbation through entrainment. This approach was applied later to various locomotion systems [5]-[7]. In addition to the studies on robotic locomotion [8], more efforts have been made to implement the neural oscillator to a real robot for various applications. Williamson showed the system that had biologically inspired postural primitives [9]. He also proposed the neuro-mechanical system that was coupled with the neural oscillator for controlling its arm [10]. Arsenio [11] suggested the multiple-input describing function technique to evaluate and design nonlinear systems connected to the neural oscillator.

Even though natural dynamic motions adapting to external changes were accomplished by the existing works, approaches for a proper behavior generation and complex task employing a robotic manipulator were not clearly described due to the difficulty of parameter tuning of a neural oscillator coupled to a mechanical system. Yang has presented simulation and experimental results in controlling the robot arm incorporating neural oscillators [12]-[14]. This work addresses how to control a real system coupled with the neural oscillator for a desired task. For this, real-time feedback is implemented to exploit the entrainment feature of the neural oscillator against unpredictable disturbances.

In the following section, a neural oscillator is briefly explained and its entrainment property is described. Details of dynamic responses and verification of developed methodology are discussed in Section III. The experimental results are presented in Section IV. Finally, conclusions are drawn in Section V.

II. Rhythmic Movement Using a Neural Oscillator

A. Matsuoka's Neural Oscillator

Matsuoka's neural oscillator consists of two simulated neurons arranged in mutual inhibition as shown in Fig. 1. [1]-[2]. If gains are properly tuned, the system exhibits limit cycle behaviours. The trajectory of a stable limit cycle can be derived analytically, describing the firing rate of a neuron with self-inhibition. The neural oscillator is represented by a set of nonlinear coupled differential equations given as

Manuscript received March 9, 2009; This work was supported by Korea MIC and IITA through IT Leading R&D Support Project. [2008-S028-01, Development of Cooperative Network-based Humanoids Technology]

W. Yang, J. Kwon, J.-H. Bae Y. Oh and B. J. You are with the Center for Cognitive Robotics Research, Korea Institute of Science and Technology, Seoul, Korea (e-mail: { wsyang, msrobot, joseph, oyh and ybj}@kist.re.kr)

N. Y. Chong is with the School of Information Science, Japan Advanced Institute of Sci & Tech, Ishikawa, Japan (e-mail: nakyoung@jaist.ac.jp)

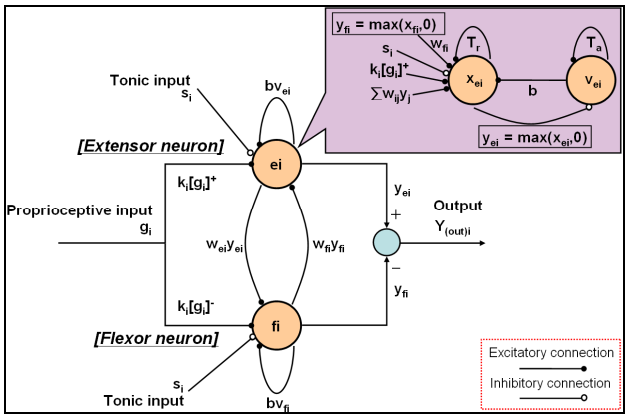

Fig. 1. Schematic diagram of Matsuoka Neural Oscillator

$$
\begin{aligned}
T_r\dot{x}_{ei} + x_{ei} &= -w_{fi}y_{fi} - \sum_{j=1}^{n} w_{ij}y_j - bv_{ei} - \sum k_i[g_i]^+ + s_i \\
T_a\dot{v}_{ei} + v_{ei} &= y_{ei} \\
y_{ei} &= [x_{ei}]^+ = \max(x_{ei},\ 0) \\
T_r\dot{x}_{fi} + x_{fi} &= -w_{ei}y_{ei} - \sum_{j=1}^{n} w_{ij}y_j - bv_{fi} - \sum k_i[g_i]^- + s_i \\
T_a\dot{v}_{fi} + v_{fi} &= y_{fi} \\
y_{fi} &= [x_{fi}]^+ = \max(x_{fi},\ 0),(i = 1,\ 2,\ \cdots,\ n)
\end{aligned}
\tag{1}
$$

where $x_{e(f)i}$ is the inner state of the i-th neuron which represents the firing rate; $v_{e(f)i}$ represents the degree of the adaptation, modulated by the adaptation constant b, or self-inhibition effect of the i-th neuron; the output of each neuron $y_{e(f)i}$ is taken as the positive part of x_i, and the output of the whole oscillator as $Y_{(out)i}$; w_{ij} (0 for $i \neq j$ and 1 for $i=j$) is the weight of inhibitory synaptic connection from the j-th neuron to the i-th neuron, and w_{ei}, w_{fi} are also weights from the extensor neuron to the flexor neuron, respectively; $w_{ij}y_i$ represents the total input from the neurons inside the network; the input is arranged to excite one neuron and inhibit the other, by applying the positive part to one neuron and the negative part to the other; T_r and T_a are time constants of the inner state and the adaptation effect of the i-th neuron, respectively; s_i is the external input, and g_i indicates the sensory input from the coupled system which is scaled by the gain k_i.

B. Coupling Neural Oscillator to Mechanical Systems

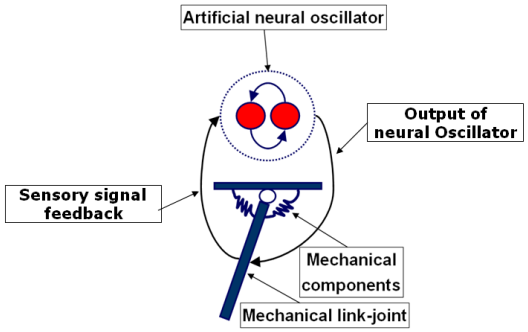

Fig. 2. Mechanical system coupled to the neural oscillator

Fig. 2 shows two types of mechanical systems connected to the neural oscillator. The desired torque signal to the i-th joint can be given by

$$\tau_i = k_i(\theta_{vi} - \theta_i) - b_i\dot{\theta}_i, \tag{2}$$

where k_i is the stiffness of the joint, b_i the damping coefficient, θ_i the joint angle, and θ_{vi} is the output of the neural oscillator that produces rhythmic commands of the i-th joint. The neural oscillator follows the sensory signal from the joints, thus the output of the neural oscillator may change corresponding to the sensory input. This is what is called "entrainment" that can be considered as the tracking of sensory feedback signals so that the mechanical system can exhibit adaptive behavior interacting with the environment.

III. Two-Link Robot Arm Control Based on Neural Oscillator

In this section, we couple the joints of a two-link robot arm to neural oscillators and propose a control method that is capable of generating an appropriate motion. The neural oscillator is a non-linear system, thus it is generally difficult to analyze the dynamic system when the oscillator is connected to it. Therefore a graphical approach known as the describing function analysis has been proposed earlier [15]. The main idea is to plot the system response in the complex plane and find the intersection points between two Nyquist plots of the dynamic system and the neural oscillator. The intersection points indicate limit cycle solutions. However, even if a rhythmic motion of the dynamic system is generated by the neural oscillator, it is usually difficult to obtain the desired motion required by the task. This is because many oscillator parameters need to be tuned, and different responses occur according to the inter-oscillator network. Hence, we describe below how to tune the parameters of the neural oscillator and implement to the real robot system.

A. Impedance Model

As shown in Fig. 3 (a), an arbitrary external force is measured by force and torque (F/T) sensor attached to the wrist joint of the robot arm. The external forces (F_x, F_y) applied to the end-effector are transformed into F_x' and F_y' of global Cartesian coordinates using a homogeneous transformation. Then the transformed external forces can be properly calculated to target trajectories in Cartesian coordinates by a virtual impedance model. The impedance model equation can be given as follows,

$$
\begin{aligned}
\ddot{x} &= -\omega_n^2 x - 2\omega_n\dot{x} + F_x' \\
\ddot{y} &= -\omega_n^2 y - 2\omega_n\dot{y} + F_y'
\end{aligned}
\tag{3}
$$

where, ω_n is the natural frequency of the impedance model.

B. Two-link robot arm coupled to neural oscillators

To implement the proposed control scheme for the two-link robot arm whose joints are coupled to neural oscillators, this subsection describes how to couple the dynamics of the robot arm and neural oscillators. The output of the neural oscillator drives the joint of the robot arm corresponding to the sensory signal input from the actuator.

The oscillator entrains the input signal so that the robot arm can exhibit adaptive behavior even under the unknown environment condition.

The dynamic equation of the robot arm coupled to the neural oscillator is given in the following form.

$$\begin{aligned} M_1\ddot{\theta}_1 + C_1\dot{\theta}_1 + (K_1 + K_T)\theta_1 - K_T\theta_2 &= K_1\theta_{v1} + K_{p1}(\theta_{d1} - \theta_1) - K_{d1}\dot{\theta}_1 \\ M_2\ddot{\theta}_2 + C_2\dot{\theta}_2 - K_T\theta_1 + (K_2 + K_T)\theta_2 &= K_2\theta_{v2} + K_{p2}(\theta_{d2} - \theta_2) - K_{d2}\dot{\theta}_2 \end{aligned} \quad (4)$$

where M_i is the inertial matrix, C_i is the Coriolis/centripetal vector, and K_i is the spring coefficient for i-th joint (i=1~2). Note that θ_{v1} and θ_{v2} are the output of neural oscillators coupled to each joint of the two-link robot arm, respectively. K_{pi} is the proportion gain and K_{di} is the differential gain for i=1~2. K_T is the virtual spring coefficient between the first and second joint.

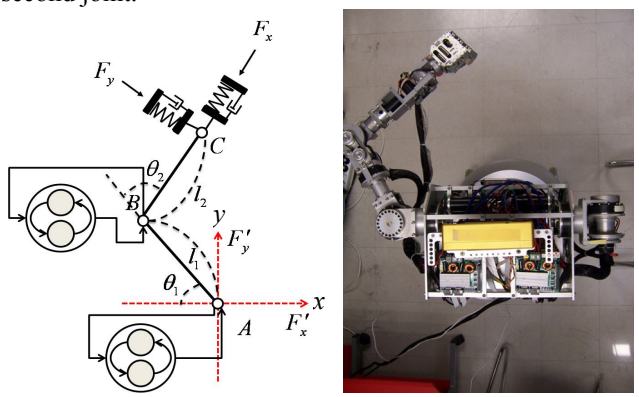

(a) (b)

Fig. 3. (a) Schematic robot arm model and (b) real robot arm coupled with the neural oscillator for experimental test

C. Control Block Diagram

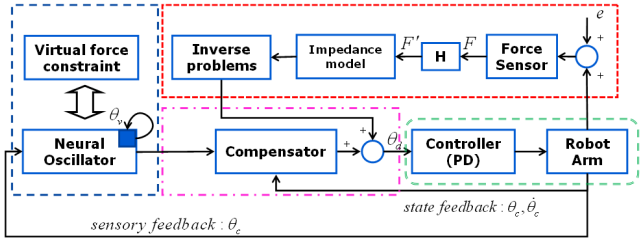

Fig. 4. The proposed control block diagram

Fig. 4 illustrates the proposed control block diagram for the neural oscillator based two-link robot arm control. In general, the artificial neural oscillator is only applicable to a particular motion such as rhythmic motions. In contrast to this, our work presents a control method to efficiently yield various motions with virtual force constraints. The virtual force constraint makes the coupled neural oscillator-robot arm possible to perform a given task compensating the reaction forces caused by the discrepancy between the desired constraint and the displacement of the end-effector. And also assuming that the difference between real reaction forces sensed by the F/T sensor and virtual forces for a desired motion is an error, e, as indicated in Fig. 4, the desired motion modified in terms of the impedance model is fed to the control command again. Finally since the neural oscillator observes and entrains intuitively the changed current status of each joint, a proper desired command θ_v can be send to the robotic system.

D. Control Stability Analysis

In general, dynamics of a robot system with n-th DOFs could be expressed as

$$H(\theta)\ddot{\theta} + \left\{\frac{1}{2}\dot{H}(\theta) + S(\theta,\dot{\theta})\right\}\dot{\theta} + g(\theta) = u, \quad (5)$$

where, H denotes the $n\times n$ inertia matrix of a robot, the second term in the right hand side of Eq.(5) stands for coriolis and centrifugal force, and the third term is the gravity effect. Then a control input for a rhythmic motion of the dynamic system shown in Eq. (5) is introduced as follows;

$$u = -C_0\dot{\theta} - J^{\mathrm{T}}(k\Delta x + \varsigma\sqrt{k}\dot{x}) - k_o\Delta\theta + g(\theta), \quad (6)$$

where

$$C_0 = \mathrm{diag}(c_1,\ c_2,\ \cdots,\ c_n)$$

$$c_i = \varsigma_0\sqrt{k}\sqrt{\sum_{j=1}^{n}\left|H_{ij}\right|},\ (i,\ j = 1,\ 2,\ \cdots,\ n)$$

$$\Delta x = x - x_d$$

$$\Delta\theta = \theta - \theta_v$$

where k and ς_0 is the spring stiffness and damping coefficient, respectively for the virtual components. C_0 is the joint damping. k_o and θ_v are the stiffness gain and the output of the neural oscillator that produces rhythmic commands, respectively.

The control input induced in Eq. (6) consists of two control schemes, those are, one is based on Virtual spring-damper Hypothesis [16]-[17] and the other is determined in terms of the output of the neural oscillator as illustrated in Eq. (4). In the control input of Eq. (6), the first term describes a joint damping for restraining a certain self-motion which could be occurred in a robot system with redundancy, and the second term means PD control in task space by using of Jacobian transpose, and also a spring and a damper in the sense of physics. Appropriate selection of joint damping factors C_0, stiffness k and damping coefficient ς renders the closed-loop system dynamics convergent, that is, x is converged into x_d and both of $\dot{x}$ and $\dot{\theta}$ are become 0 as time elapses. In general, the neural oscillators coupled to the joints perform the given motion successively interacting with a virtual constraint owing to the entrainment property, if gains of the neural oscillator are properly tuned [12]-[13]. In the proposed control method, the virtual force constraint is considered as a virtual guide for generating a desired motion. Also, the coupled model enables a robotic system to naturally exhibit a biologically inspired motion employing sensory signals obtained from each joint under an unpredictable environment change.

Then, closed-loop dynamics with Eq. (5) and Eq. (6) is expressed as

$$H(\theta)\ddot{\theta}+\left\{\frac{1}{2}\dot{H}(\theta)+S(\theta,\dot{\theta})+C_0\right\}\dot{\theta}+J^{\mathrm{T}}(k\Delta x+\varsigma\sqrt{k}\dot{x}) \quad (7)$$
$$+k_o\Delta\theta=0$$

The inner product between $\dot{\theta}$ and the closed-loop dynamics of Eq. (7) yields

$$\dot{\theta}^T\left[H(\theta)\ddot{\theta}+\left\{\frac{1}{2}\dot{H}(\theta)+S(\theta,\dot{\theta})+C_0\right\}\dot{\theta}+J^{\mathrm{T}}k\Delta x+J^{\mathrm{T}}\varsigma\sqrt{k}\dot{x}\right.$$
$$\left.+k_o\Delta\theta\right]=0 \quad (8)$$

and

$$\frac{\mathrm{d}}{\mathrm{dt}}E=-\dot{\theta}^TC_0\dot{\theta}-\dot{x}^{\mathrm{T}}\varsigma\sqrt{k}\dot{x}\le 0, \quad (9)$$

where E stands for the total energy

$$E(\dot{\theta},\,\Delta x,\,\Delta\theta)=\frac{1}{2}\dot{\theta}^TH(\theta)\dot{\theta}+\frac{k}{2}\|\Delta x\|^2+\frac{k_o}{2}\|\Delta\theta\|^2 \quad (10)$$

In Eq. (10), the first term of the quantity E describes the kinetic energy of the robot system, the second term means an artificial potential energy caused by the error Δx in task space and the error $\Delta\theta$ gives rise to an artificial potential energy corresponding to the third term in joint space. As it is well known in robot control, the energy balance relation of Eq. (9) shows that the input-output pair $(u, \dot{\theta})$ related to the motion of Eq. (8) satisfies passivity.

IV. Experimental Verifications

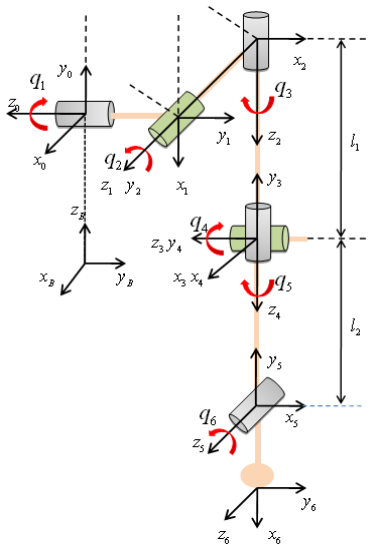

Fig. 5. Schematic figure for D-H parameter of the robot arm

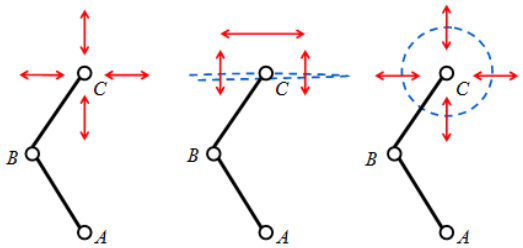

(a) (b) (c)

Fig. 6. The given tasks of the two-link robot arm. The dashed lines are the desired motions. The arrows indicate the direction which an unknown external force is applied to the end-effector of the robot arm

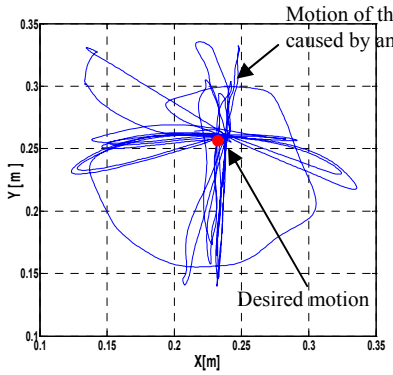

(a)

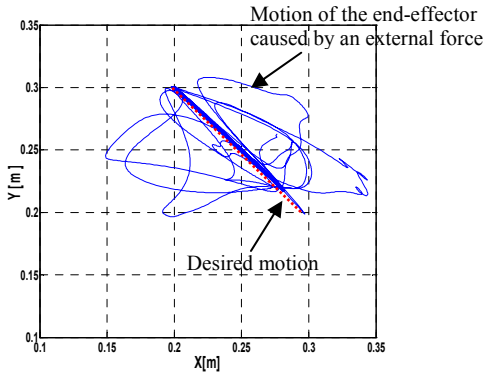

(b)

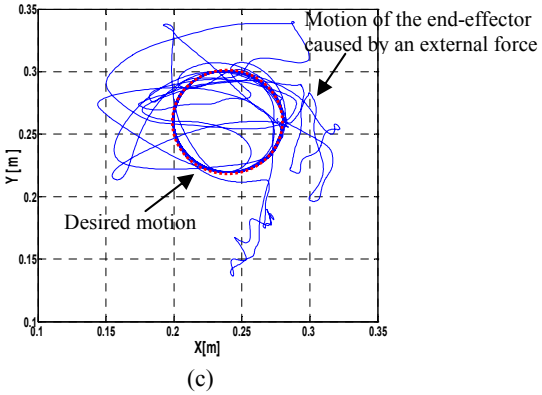

(c)

Fig. 7. The trajectories drawn by the end-effector of the real robot arm

For considering the possibility of the proposed control scheme described in Section III, a real robot arm with 6 degrees of freedom (see Fig. 3 (b)) are employed and a real time control system is constructed. This arm controller runs at 200Hz and is connected via IEEE1394 for data transmission

at 4kHz. ATI industrial automation's Mini40 sensor was fitted to the wrist joint of the arm to detect external disturbances. The appropriate parameters in Table I were used for the neural oscillator. Also Table I illustrates the parameters on the arm dynamics of the real robot. Figure 5 shows the arm kinematics of the real robot arm. Since the desired motions are generated in the horizontal plane, q_1 and q_3 are set to 90°. The initial values of q_5 and q_6 are set to 0°, respectively. q_2 and q_4, corresponding to θ_1 and θ_2 in Fig. 3 (a), respectively, are controlled by the neural oscillators. We performed extensive experiments to evaluate the proposed control scheme described in section III. Various tasks in cases 1 through 3 of Figure 6 (a), (b) and (c) are verified with respect to adaptive motion of the arm against arbitrary forces.

Figure 7 (a) to (c) indicates experimental results on case 1 to case 3 of Figure 6, respectively. Through these cases, we examine whether various desired motions such as motionless status, linear and circular motions can be attained or not. Basically kinds of these motions were verified from the results of Fig. 7. In Figure 7, the dotted lines in the center part of the figure show the desired motions and overlapping lines illustrate the motion trajectories that are drawn in terms of the end-effector of the real robot arm. In addition, we pushed and pulled the end-effector along the positive and negative x direction as shown in Figure 7 (a). And such conditions were also applied to the robot arm along the y direction in order to evaluate an adaptive feature of the proposed control method under additive external disturbances. It can be verified from the experimental result of Fig. 7 (a) that the robot arm is moved well according to the direction of the applied force (about 10 N and below). If an arbitrary force exists, it follows that the end-effector of the robot arm shows a compliant motion even in the linear motion and circular motion of the robot arm as seen in Figs. 7 (b) and (c).

The force and torque (F/T) sensor value in the x and y direction are added to equation (3). Then, the joint angles change according to the direction of the impact of the force induced by the collision, which makes the neural oscillators entrain the joint angles for biologically inspired motion. Hence a change in the output produced intuitively from the neural oscillator causes a change in the joint torque. Finally the joint angles are modified adequately. Thus, it can be confirmed that the proposed neural oscillator based robot arm control approach successfully dealt with unexpected collisions sustaining desired motions.

V. Case Study: Opening and Closing a Drawer

A. Experimental System

Figure 8 conceptually illustrates the objective tasks with experimental setup for validation of the proposed control scheme. We evaluate the entrainment capability of the neural oscillator that enables a manipulator to implement and sustain the given task under various environmental changes. Hence, in order to verify the possibility of such adaptation performance, we apply various circumstances to the coupled oscillator-robot arm with the tasks with respect to opening and closing a drawer as seen in Fig. 8. A drawer can give the constraint condition for performing the given task such as opening or closing to the proposed control architecture without making a constraint condition by intention. This is why we consider the task as the case study of this work in order to experimentally verify the neural oscillator based control method.

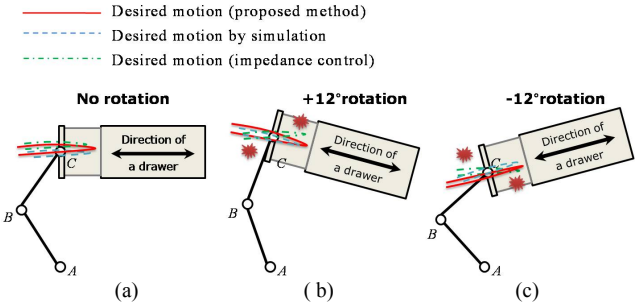

Fig. 8. Schematic figure on the experiments that robot arm opens and closes a drawer repeatedly. (a) fix the drawer in accordance with the robot arm motion, (b) rotate the drawer clockwise about 12°, (c) rotate the drawer counter-clockwise about 12°

We tightly joined the end-effector of the robot arm to the drawer. The end-effector's direction of the robot arm is designed in accordance with the direction to open or close the drawer under the condition that the drawer is not rotated but fixed. In Figs. 8 (b) and (c), the drawer was rotated clockwise and counter-clockwise about 12° for considering unknown environmental changes. Then, the end-effector of the robot arm brings about various collision problems with the drawer due to a different direction between the end-effector of the robot arm and the drawer. Consequently, the proposed method based on the neural oscillator shows successfully adaptive motion against uneven disturbances such as the collision. Now, we will examine what happens in the arm motion on performing the objective task if additive external disturbances exist. Table I describes the parameters set within a limit cycle stable range for incorporating the neural oscillators to a robotic system [13]-[14].

TABLE I
Parameters of the Neural Oscillator & Robot Arm Model

Initial parameters			
Neural oscillator(1)		Neural oscillator(2)	
Inhibitory weight (w_1)	1.7	Inhibitory weight (w_2)	1.7
Time constant (T_{r1})	0.68	Time constant (T_{r2})	0.7
(T_{a1})	1.36	(T_{a2})	1.4
Sensory gain (k_1)	3.1	Sensory gain (k_2)	15.6
Tonic input (s_1)	1.0	Tonic input (s_2)	1.0
Robot Arm Model			
Mass 1 (m_1), Mass 2 (m_2)		2.347kg, 0.834kg	
Inertia 1 (I_1), Inertia 2 (I_2)		0.0098kgm^2, 0.0035kgm^2	
Length 1 (l_1), Length 2 (l_2)		0.224m, 0.225m	

B. Experimental Results

Figures 9 and 10 illustrate the experimental results on each joint output of the robot arm as the sensory feedback of the neural oscillator is turned off and on, respectively. In the first case of Fig. 8 (a), the desired motion of robot arm is not changed owing that the drawer is immovable during 0s to 20s.

The first joint (q_2) and the second one (q_4) are actuated to move to the distance corresponding to an external force using Eq. (3) as explained in above section III. Hence, if the drawer rotates about +12° and -12° as illustrated in Figs. 8 (b) and (c) during 20s to 40s and 40s to 60s, the robot arm's motion is autonomously altered. In Figs. 9 and 10, the blue lines indicate the desired trajectories produced by means of the neural oscillators for the joints 1 and 2. The red dotted lines are the output of the joints 1 and 2 that is changed in terms of forces applied when the drawer is rotated. Comparing the result of Fig. 9 with the neural oscillator based control (see Fig. 10), if the sensory information is fed again, it can be observed that the outputs of each joint and neural oscillator are changed whenever unknown disturbances are induced into the robot arm. Such the effect could be accomplished owing that the oscillator based control reproduces the desired joint input entraining the joint motion coupled with the neural oscillator through sensory feedback. Figure 11 shows the snap shots of the robot arm controlled by impedance control. The snap shots in Fig. 12 show the motion of the robot arm implementing the proposed control approach based on the neural oscillator, where we can observe that the end-effector traces the rotated drawer direction.

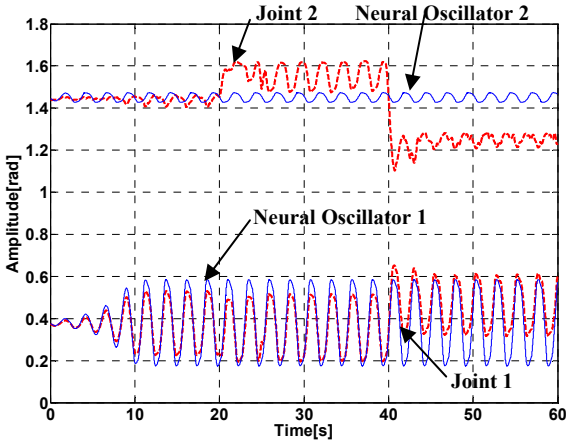

Fig. 9. The outputs of each joint and neural oscillator as the sensory feedbacks of the neural oscillators are turned off.

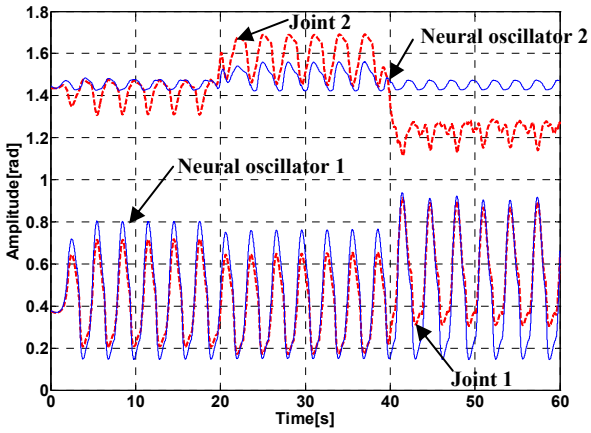

Fig. 10. The outputs of each joint and neural oscillator as the sensory feedbacks of the neural oscillators are turned on.

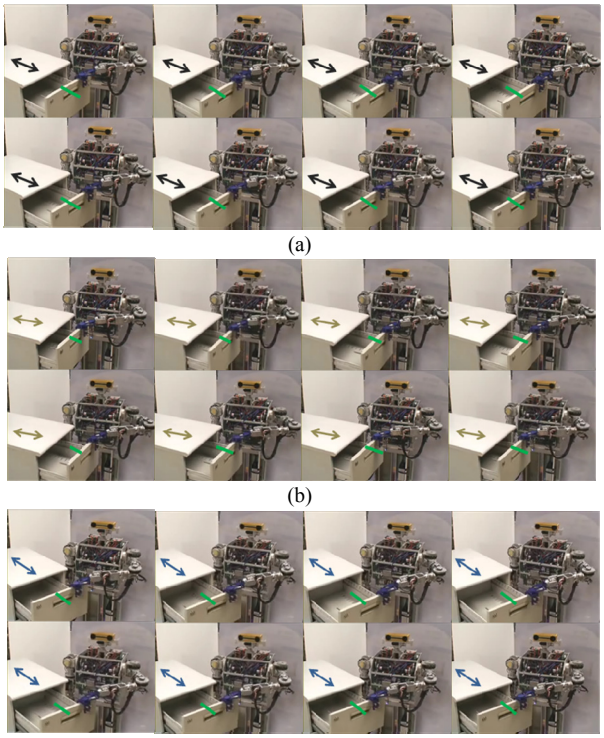

Fig. 11. Snap shots of the robot arm motions when sensory information isn't fed again in cases of 0° (a), -12° (b) and 12° (c) rotation of the drawer

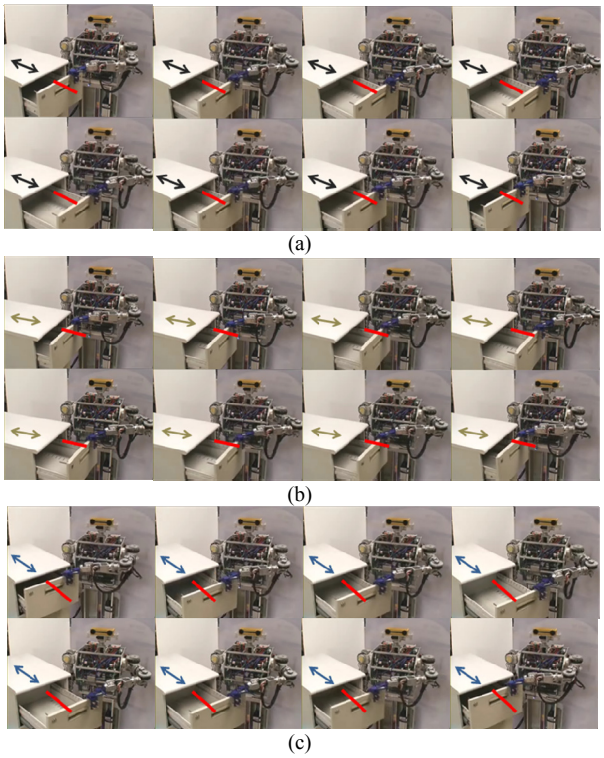

Fig. 12. Snap shots of the robot arm motions when sensory information is fed again in cases of 0° (a), -12° (b) and 12° (c) rotation of the drawer

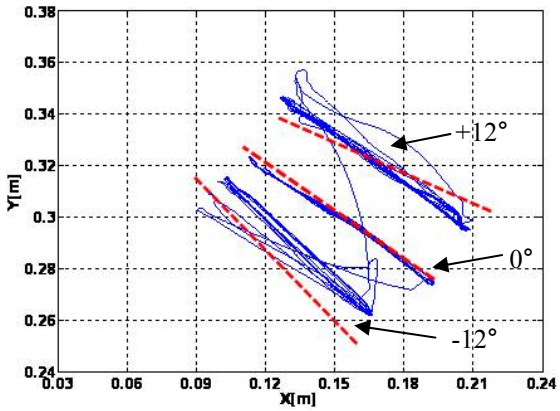

Fig. 13. Trajectories of the end-effector of the robot arm in case that the sensory feedbacks of the neural oscillator are turned off

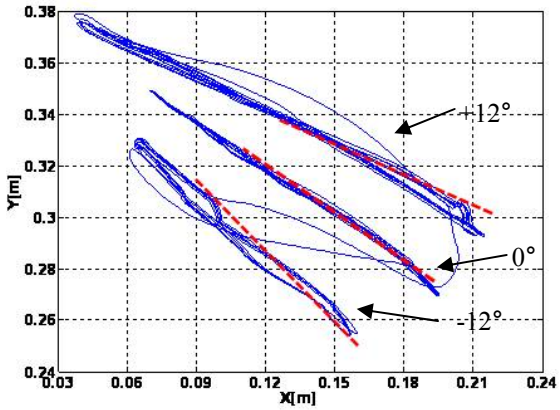

Fig. 14. Trajectories of the end-effector of the robot arm in case that the sensory feedbacks of the neural oscillator are turned on

As shown in Figs 13 and 14, the end-effector of the robot arm draws the trajectories corresponding to the desired motion for opening and closing the drawer. The straight dotted lines indicate the desired trajectories of the robot arm generated by simulation. The blue lines show the trajectories measured at the end-effector of the robot arm in experiments related with Figs. 11 and 12. In Fig. 13, movements of the robot arm are identical with the expected performance although there are inefficient motions due to unknown disturbances. This is because that the desired input of each joint is modified adequately by the impedance model (see Fig. 4) measuring external forces with the F/T sensor even though sensory information of the neural oscillators isn't fed again. In comparison with this, the individual trajectories drawn by the robot arm in figure 14 are completely consistent with the rotated direction of the drawer. Thus, the robot arm coupled with the neural oscillator exhibits the superior potential in adaptive motion exploiting the sensory feedback of the neural oscillator for the capability of entrainment. From experiment results of Figs 10, 12 and 14, the measured trajectories and movements of real robot arm imply that the neural oscillator enables the robot arm to exhibit the self-adapting motion to enhance adaptive motion sustaining the objective task and motion stability.

For showing the superiority of the biologically inspired control approach, we perform more complex task employing 6-DOF motion of the robot arm. Fig. 15 shows the behavior of the robot arm with respect to opening a door. In the same manner, the task can be attained simply regardless of the desired motion generation for each joint of 6-DOF robot arm coupled with neural oscillators. Because the arm is so compliant, the tracking error is absorbed in the arm compliance. Thus, the robot can open the door easily even in a imprecise desired motion by the mechanical constraint between the door and the end-effector of the robot arm as seen in Fig. 15. In addition, though a desired task changes unexpectedly, the entrainment function of the neural oscillator adjusts the control commands in an adaptive way so as to maintain given movements.

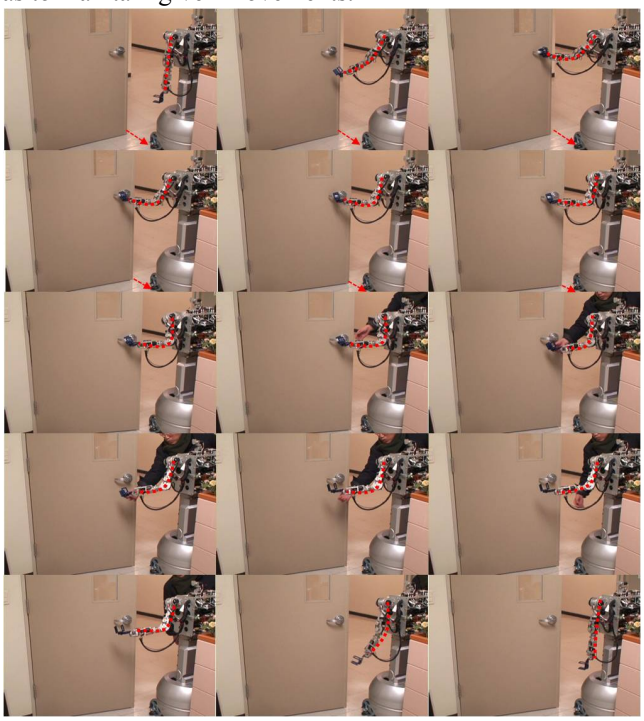

Fig. 15. Snap shops of 6-DOF robot arm motion in experiment of opening a door

VI. Conclusion

We have presented an example of human-like behavior of a planar robot arm whose joints were coupled to neural oscillators. In contrast to existing works that were only capable of rhythmic pattern generation, our approach allowed the robot arm to trace a trajectory correctly through entrainment. For achieving this, we proposed that the robot arm model coupled with neural oscillators can exhibit natural rhythmic motions, which entrains unknown disturbances with sensory information. This causes appropriate desired motions irrespective of precisely modelling with respect to external disturbances. For such reason, it was observed from experimental results of the coupled robotic system that the novel adaptive motions corresponding to an external force measured by the FT sensor values clearly appear. This approach will be extended to a more complex behavior in

three-dimension toward the realization of biologically inspired robot control architectures Also, theoretical analysis on the coupled oscillator-mechanical system will be extended as controllers.

REFERENCES

[1] K. Matsuoka, "Sustained Oscillations Generated by Mutually Inhibiting Neurons with Adaptation," *Biological Cybernetics*, Vol. 52, pp. 367-376 (1985).

[2] K. Matsuoka, "Mechanisms of Frequency and Pattern Control in the Neural Rhythm Generators," *Biological Cybernetics*, Vol. 56, pp. 345-353 (1987).

[3] G. Taga, Y. Yamagushi and H. Shimizu, "Self-organized Control of Bipedal Locomotion by Neural Oscillators in Unpredictable Environment," *Biological Cybernetics*, Vol. 65, pp. 147-159, (1991).

[4] G. Taga, Y. Yamagushi and H. Shimizu, "Self-organized Control of Bipedal Locomotion by Neural Oscillators in Unpredictable Environment," *Biological Cybernetics*, Vol. 65, pp. 147-159, (1991).

[5] G. Taga, "A Model of the Neuro-musculo-skeletal System for Human Locomotion," *Biological Cybernetics*, Vol. 73, pp. 97-111 (1995).

[6] S. Miyakoshi, G. Taga, Y. Kuniyoshi, and A. Nagakubo, "Three-dimensional Bipedal Stepping Motion Using Neural Oscillators-Towards Humanoid Motion in the Real World," *Proc. IEEE/RSJ Int. Conf. on Intelligent Robots and Systems*, pp. 84-89 (1998).

[7] Y. Fukuoka, H. Kimura and A. H. Cohen, "Adaptive Dynamic Walking of a Quadruped Robot on Irregular Terrain Based on Biological Concepts," *The Int. Journal of Robotics Research*, Vol. 22, pp. 187-202 (2003).

[8] G. Endo, J. Nakanishi, J. Morimoto and G. Cheng, "Experimental Studies of a Neural Oscillator for Biped Locomotion with QRIO," *Proc. IEEE/RSJ Int. Conf. on Intelligent Robots and Systems*, pp. 598-604 (2005).

[9] M. M. Williamson, "Postural Primitives: Interactive Behavior for a Humanoid Robot Arm," *4th Int. Conf. on Simulation of Adaptive Behavior*. MIT Press, pp. 124-131 (1996).

[10] M. M. Williamson, "Rhythmic Robot Arm Control Using Oscillators," *Proc. IEEE/RSJ Int. Conf. on Intelligent Robots and Systems*, pp. 77-83 (1998).

[11] A. M. Arsenio, "Tuning of neural oscillators for the design of rhythmic motions," *Proc. IEEE Int. Conf. on Robotics and Automation*, pp. 1888-1893 (2000).

[12] W. Yang, N. Y. Chong, C. Kim and B. J. You, "Optimizing Neural Oscillator for Rhythmic Movement Control," *Proc. IEEE Int. Symp. on Robot and Human Interactive Communication*, pp. 807-814 (2007).

[13] W. Yang, N. Y. Chong, Jaesung Kwon and B. J. You, "Self-sustaining Rhythmic Arm Motions Using Neural Oscillators," *Proc. IEEE/RSJ Int. Conf. on Intelligent Robots and Systems*, pp. 3585-3590 (2008).

[14] W. Yang, N. Chong, C. Kim and B. J. You, "Entrainment-enhanced Neural Oscillator for Rhythmic Motion Control," *Journal of Intelligent Service Robotics*, Vol. 1, pp. 303-311 (2008).

[15] Jen-Jacques E. Slotine, Weiping Li, "Applied Nonlinear Control," Englewood Cliffs, N. J., Prentice Hall. (1991).

[16] S. Arimoto, M. Sekimoto, H. Hashiguchi and R. Ozawa, "Natural Resolution of ill-Posedness of Inverse Kinematics for Redundant Robots: A Challenge to Bernstein's Degrees-of Freedom Problem," *Advanced Robotics*, 19: 401-434 (2005).

[17] S. Arimoto, M. Sekimoto, J.-H. Bae and H. Hashiguchi, "Three-dimensional Multi-Joint Reaching under Redundancy of DOFs," *Proc. IEEE/RSJ Int. Conf. on Intelligent Robots and Systems*, 1898-1904 (2005).